MRP File No. 47-1688/10 (WRO)

Title of Minor Research Project

"Structural & Electrical Studies of Strontium doped Lead Titanate"

Date of Sanction
March 16, 2011
Date of Completion
March 15, 2013

Principle Investigator
Dr. Bajpeyee A. U.

Institute
Department of Physics
Arts Commerce and Science College, Kiran Nagar,
Amravati (Maharashtra) 444606

Highlighted ingredients of the Principle Investigator are available at webpage
www.narsammaacsc.org AND www.vishwabharati.ac.in
Correspondence at aubajpeyee@gmail.com or +91-9422157797, +91-0721-2540793

1.1 Introduction

Cellular phone technology in particular and wireless technology in general demands cheaper, compact and more condensed electronic circuitry with more extended functionality of the devices. This can be achieved by developing innovative electronic materials especially dielectric materials for memory storage, components and designing of it into the devices. These dielectric materials are used as a capacitor. The capacitors in random access memories (RAMs) have traditionally been fabricated by controlled oxidation of the free surfaces of the silicon integrated circuit. This produces a strong, chemically stable reliable thin-thick film capacitor, but it has a disadvantage of producing smaller dielectric constant (~6).

Our pre knowledge tells us that, the capacity of a parallel plate condenser is directly proportional to its surface area and dielectric constant of the material kept between two plates. Using simple calculations for this, suppose, a material with 100 times the dielectric constant is required to be synthesized, the required surface area would be 100 times smaller. With this view, a planar technology with fewer processing steps and higher yields; or alternative new material could be combined to make possible huge multi-Gbit memories i.e. either SiO_2 capacitors or a combination of SiO_2 and Si_3N_4 nitride, which is termed oxy-nitride. RAMs was also intended to utilize Ta_2O_5 (Tantalum oxide with dielectric constant ~ 25). But, it appears that the RAM evolution skipped intermediate stage and has passed directly to very high dielectric materials (500–1500) that are ferroelectric or nearly ferroelectric. Many of ferroelectric materials are oxides of the ABO_3 perovskite family. A good review of this technology and its development is given by Gnade et al.[1] and Kotecki [2]. Along the same line Tasch, Parker and Mochizuki [3] focused attention on the prospect of using high dielectric-ferroelectric films for DRAM capacitors.

At this stage of development of planer technology, the processing problems of integrating high dielectric perovskite oxides as thin-film capacitors into microelectronic devices had already been solved to some extent. At the same time thick film technology should not be ignored due to its special features in the development of the current electronic, microelectronic and computer based technology. In order to have it accounted, literature is reviewed. The literature supports the investigations and further work for the development and in the

experimentation of the thick films due to its constantly demanding applications. The term 'thick film' does not merely relate so much to the thickness of the film but more to the kind of deposition. Thick films can be deposited by low-priced processing methods. Hence, it came into force with the dielectric, paraelectric, piezoelectric and ferroelectric properties to manage the commercial demands in the memory based industries and tools designed for human endeavor [4]. Dielectric properties can be increased with the increasing density of the materials which urge the requirements of the thick film and its applications. The properties of dielectric materials in the form of pastes to be deposited as a thick film, necessary for multilayer applications, have not been studied so extensively [5]. Hence, thick film deposition by using screen printing technique is adopted here.

1.2 Advantages of lead titanates

Lead titanate is a well-known ferroelectric perovskite material with high Curie point and moderate dielectric constant. When it is modified with the dopants like calcium and strontium it can be used as an attractive high dielectric constant material.

Its dielectric properties are of much advantage. It is used in piezoelectric system and can be constructed for transducer, generators, sensors, actuators. Lead titanates are also used in just principled in a contact microphone, a sensor converts a physical parameter such as acceleration or pressure into an electrical signal.

It is used in sonar waves also used in actuators to convert an electrical signal into a precisely controlled physical displacement to finely adjust precision machining tools, lenses or mirrors and to control hydraulic valves which acts as small volume pumps or special-purpose motors and in other applications.

It is used in loudspeakers, used to control precisely the distance between mirrors in the laser electronics to get accurately maintained optical conditions inside the laser cavity. Its piezoelectric property is used to generate ultrasonic vibrations for cleaning.

Important is that, ferroelectric lead titanate films, grown directly on a semiconductor such as Si, form a very promising combination for nonvolatile memory devices applications [6, 7].

1.3 Need of present investigation

Lead based titanates are commonly, easily available, of low cost and used with different compositions and dopants, due to which its piezoelectric coefficients, dielectric permittivity, ferroelectricity, etc can be increased. Its increasing success at this remarkable level more and more showed the way to pull towards lead based titanates mainly in the form of dopants in lead titanate. Though lead based titanates has environmental repercussions and sensible toxicity, it is worth mentioning here that when its scientific applications in the current DRAM technology is noticeable, it is found that it can be studied further for the contribution in the current electronic world and to get enhancement in the properties.

Thus, it is decided from the knowledge of its advantageous applications in the current compact technology, its easy availability, its dielectric properties with high dielectric constant on doping, its ferroelectric properties used for non-volatile memories and its overall scientific applications, to work for the lead titanates in the film form.

Hence, study of the structural and electrical characterizations of its dielectric layers on semiconductor silicon is presented in this project.

2.1 Synthesis of Lead Titanates

2.1.1 Chemicals and weighing

The basic precursor chemicals as a raw material used in this method and its molar concentration is depicted in the table 1 to 3.

Molecular Weights of Chemicals used	
Chemicals	**Molecular Weights**
$Pb(NO_3)_2$ in gm. wt.	331.208
$Sr(NO_3)_2$ in gm. wt.	211.628
$TiCl_4$ in ml.	346.195
HNO_3 in ml.	063.010

Table 1: Molecular Weights of Chemicals used

Un-doped $PbTiO_3$ (PT)	
Chemicals	**Net amount**
$Pb(NO_3)_2$ in gm. wt.	16.5000
$TiCl_4$ in ml.	17.309
HNO_3 in ml.	12.62

Table 2: Weighed chemicals used for un-doped PT

Molar Concentration for $Pb_{1-x}Sr_xTiO_3$ (PST) $TiCl_4$ = 10 ml, HNO_3 = 8.88 ml				
X concentration In gram/mole of Sr	30%	40%	50%	60%
$Pb(NO_3)_2$ in gm. wt.	11.5929	9.9362	8.2802	6.6024
$Sr(NO_3)_2$ in gm. wt.	3.1744	4.2325	5.2907	6.3489

Table 3: Weighed chemicals used for Sr doped PT

2.1.2 Chemical Reaction for the synthesis

Advantageous Wet Chemical Method with the modification for Synthesis of Mixed-Metal Oxide over solid-state reaction [8-10] is finally adopted.

$Pb(NO_3)_2 + TiCl_4 + 4HNO_3$???????? intermediate stage ???????????

$PbTiO_3 + 6NO_2$ (g)? + $1.5O_2$ (g)? + 4HCl (g)?

---------- **1**

(1-x) $Pb(NO_3)_2$ + x $A(NO_3)_2$ + $TiCl_4$ + $4HNO_3$???????? intermediate stage ??????????? $Pb_{(1-x)}A_{(x)}TiO_3 + 6NO_2$ (g)? + $1.5O_2$ (g)? + 4HCl (g)?

---------- **2**

(1-x) $Pb(NO_3)_2$ + x $Sr(NO_3)_2$ + $TiCl_4$ + $4HNO_3$???????? intermediate stage ??????????? $Pb_{(1-x)}Sr_{(x)}TiO_3 + 6NO_2$ (g)? + $1.5O_2$ (g)? + 4HCl (g)?

---------- **3**

2.1.3 Grinding, Mixing and stirring

PT: As mentioned molar concentration of the $Pb(NO_3)_2$, precursor powder has been grounded well in the mortar to get homogeneity. The precursor powder is then taken into the borocil glass beaker of 500 ml volume capacity. $TiCl_4$ and HNO_3 are added simultaneously into it by injection method to form a yellowish white solution. This solution is then stirred at 100°C for 2 hour to get dried precipitate with white colour which is an intermediate stage of reaction proposed. The powder so obtained is weighed again to find the percentage productivity of the reaction mechanism carried out as depicted in table 4. With this a white coloured raw powder is obtained, after calcination treatments it results into $PbTiO_3$ (PT). PST: With as mentioned molar concentrations of the $Pb(NO_3)_2$ and $Sr(NO_3)_2$ powder same process of the formation of the PCT i.e. calcium doped lead titanate is followed to get white coloured doped $PbTiO_3$ (PST) i.e strontium doped lead titanate powder as depicted in table 4. The process is used for all compositions.

2.1.4 Powder preparation

Homogeneous powder with an attempt to reduce the size of the particles by means of calcinations (annealing in the air) treatments was equally divided into three parts and accordingly coded.

Calcination Temperature	**600°C**	**700°C**	**800°C**
	Coding		
Pure $PbTiO_3$	PT600	PT700	PT800
% Sr doping in Lead Titanate			
30% Sr: Coding	3PST600	3PST700	3PST800
40% Sr: Coding	4PST600	4PST700	4PST800
50% Sr: Coding	5PST600	5PST700	5PST800
60% Sr: Coding	6PST600	6PST700	6PST800

Table 4: Coding system wrt calcination temperatures and varying molar concentrations

2.2 Structural and Electrical Characterizations

2.2.1 X-Ray Diffraction Study (XRD)

X-ray diffraction technique is used as a structural characteristic to study the samples in the form of powder prepared. XRD patterns of all the powder samples are studied and then analyzed and phase is confirmed. X-ray diffraction of the (111) silicon wafer is also provided. The phase conversion ratio and crystallite size is calculated, its variation with temperature is studied. Peaks were matched with the peaks in JCPDS data card file and discussed. Crystallite size and c/a ratio for lattice anisotropy is calculated and reported.

Figure 1, shows XRD patterns of pure lead titanate, $PbTiO_3$ (PT) calcined at 450°C, 600°C, 700°C and 800°C. Patterns are indexed at their major peak positions. It confirms formation of tetragonal phase. The average crystallite size was calculated from the experimental XRD peaks by using Debye-Scherer equation [11 -13].

? ? $\frac{? O}{E ???T}$ ---------- **3.1**

Where, β is the full width at half-maximum intensity (FWHM in radians) of a peak at an angle ?; K is a constant (0.9); ? (1.54060 A.U.) is the wavelength of the X-ray source. Unknown peaks other than indexed are observed in XRD pattern for PT prepared.

The diffraction pattern of the silicon substrate utilized to deposit the layers of dielectric materials by screen printing technique [14-16] is experimentally carried out successfully. The (111) orientation of the silicon crystal is confirmed from JCPDS card file no. 01-77-2110 and 01-77-2109. The substrates are in the form of wafer having uniform thickness of about 850 μm was used for the purpose of the printing.

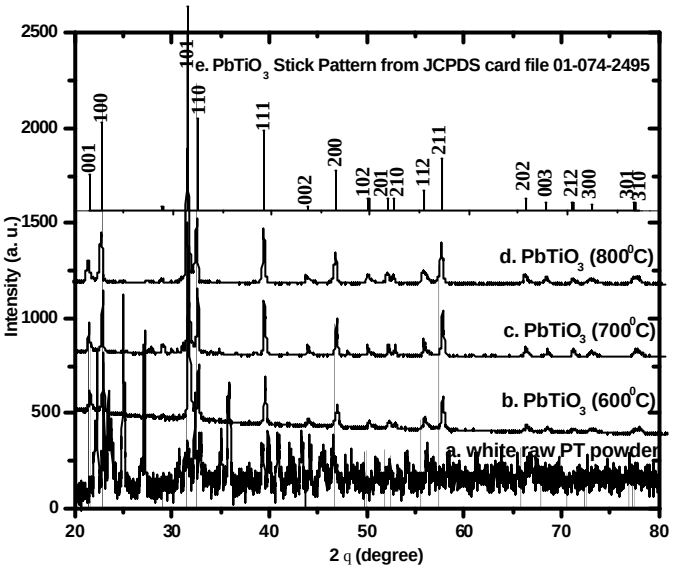

Figure 1: X-Ray Diffraction Patterns of undoped $PbTiO_3$ annealed at a) 450°C b) 600°C, c) 700°C, d) 800°C and e) stick pattern for $PbTiO_3$

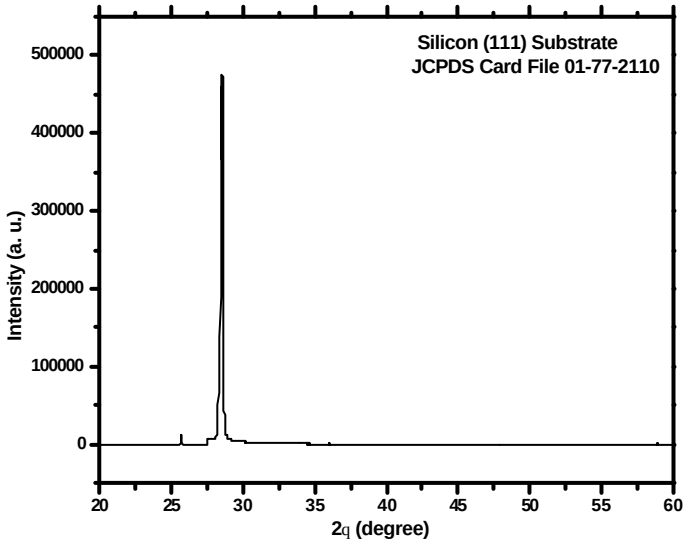

Figure 2: XRD pattern of (111) Silicon

XRD of the synthesized material calcined at 450^{o}C is shown in figure 1 (a). It shows formation of the intermediate compound along with the peaks for $PbTiO_3$ which suggests beginning of its formation. The XRD patterns for the compound calcined at higher temperatures confirm the formation of $PbTiO_3$. The XRD patterns for samples calcined at 600^{o}C, 700^{o}C and 800^{o}C are provided in Fig. 3.1 (b-d) with standard data reported as shown in Figure 1 (e). Diffraction peaks were confirmed from respective JCPDS card files as presented in table 5. The calculated average crystallite size D [17] is presented in table. The corresponding peaks were indexed.

Calcination Temperature	**Products**
450^{o}C	Homogeneous raw white PT powder including 1. Lead oxide hydrate JCPDS file No. 72-2395 2. Lead oxide hydroxide JCPDS file No. 77-1895 3. Titanium aqua oxide hydroxide JCPDS file No. 38-0700 4. Titanium dioxide JCPDS file No. 21-1276 5. $PbTiO_3$ (Lead Titanate) JCPDS file No. 74-2495 6. $PbTiO_3$ (Lead Titanate) JCPDS file No. 75-0438 7. $PbTiO_3$ (Lead Titanate) JCPDS file No. 03-0721 8. $PbTiO_3$ (Lead Titanate) JCPDS file No. 06-0452
600^{o}C	$PbTiO_3$ (Lead Titanate) JCPDS file No. 01-074-2495
700^{o}C	
800^{o}C	

Table 5: Final products and corresponding calcination temperatures

It is observed that the resultant product consists of variety of agglomerated particle size depending on calcination conditions also [18].

The calcination temperature less than 450^{o}C are not useful as it shows formation of intermediate phase and incomplete product. The minimum calcination temperature 600^{o}C is observed to be required to form $PbTiO_3$. Most of the organic residue is removed at this temperature.

Thus, XRD investigation of materials suggests formation of tetragonal structure of $PbTiO_3$. The c/a ratio which is the parameter that governs the ferroelectric property of $PbTiO_3$ is also listed in Table 6.

Calcination Temperature	2q (degree)	FWHM (B)	Crystallite Size (nm)	Average (nm)	% Phase Conversion ratio
600°C	22.7692	0.1719	82.27	71.63	99.88
	31.4859	0.2197	65.97		
	32.4223	0.2104	66.64		
700°C	22.7658	0.1335	105.92	97.15	93.89
	31.4638	0.1685	85.48		
	32.4249	0.1435	100.06		
800°C	22.7233	0.1357	82.29	72.32	77.35
	31.4786	0.2990	66.03		
	32.3980	0.1843	68.64		

Table 6: Calcination temperature, average crystallite size and % phase conversion ratio

Calcination temperature for $PbTiO_3$	Lattice Parameters		Tetragonality	% Phase Conversion ratio
	c	a	c/a	
JCPDS card	4.15	3.9	1.06410	
600°C	4.14242	3.90234	1.06152	99.76
700°C	4.14384	3.91013	1.05977	99.59
800°C	4.11818	3.90293	1.05515	99.15

Table 7: Calcination temperature, c/a and % phase conversion

2.2.2 Phase conversion ratio

The XRD peaks corresponding to diffraction planes (101), (110), (100), (001), (200) and (211) which ascribed to tetragonal $PbTiO_3$ phase were chosen for determination of phase conversion ratio. The conversion % of the $PbTiO_3$ phase at different calcination temperatures were listed in table 7. It was estimated qualitatively from XRD results and from the formula 3.2.

The percentage phase conversion ratio of the lead titanate nano-powders calculated from experimental XRD results to the standard values from JCPDS card file no. 01-074-2495 for synthesized material was estimated [19, 20]. It is recorded for the first three strongest lines of the experimental as well as standard data.

? ????? ?????????? ? $\frac{?_?}{?_?? ?_?? ?_?}$? ??? ---------- **3.2**

Where, $I_1(101)$, $I_2(110)$ and $I_3(100)$ are the relative intensities corresponding to 1st, 2nd and 3rd maximum peaks. At the room temperature, nano-crystalline PT powder has major peak at (101) which belongs to the tetragonal phase with cell parameters a = b = 3.900 A^0 and c = 4.150 A^0 of space group P4mm in JCPDS card file, experimentally calculated values at calcination temperature 600°C is a = b = 3.90234 A^0 and c = 4.14242 A^0. Phase conversion ratio results in tetragonal phase of $PbTiO_3$ system. Percentage phase conversion for the powders calcinated at 700°C and 800°C is also up to the mark. Thus, percentage phase conversion and purity of synthesized material supports the reaction mechanism and the reaction proposed. It confirms synthesis steps for further processing of doped PT powders, these steps used in the process is generalized to synthesis of the pure lead titanate with a modification. This knowledge primarily may help in realizing dielectric property and this nature of the nano-structured powders to be used for the deposition of dielectric layers on the silicon (111) substrates will be explored in the forwarding section of this project.

After confirmation from XRD for pure PT, lattice constants at different calcination temperatures are calculated. Tetragonal structure is confirmed from JCPDS files. The c/a ratio is calculated using (001) plane (lattice constant c) and (100) plane (lattice constant a = b). Table 7 shows the c/a ratio against calcination temperature values. The tetragonallity index is observed higher for the 600^0C temperature relative to other two calcination temperatures. Variation in the calcination temperature affects obtained average crystallite sizes and the c/a ratio of PT, reported that it is related with Pb/Ti ratio and level of formation of the extra PbO phase [21] which needs some investigations.

The results of tetragonality from intensity ratio as per formula 3.2 are compared with the calculations from c/a ratio. It is found in agreement for the PT powder calcined at 600°C and get deviated for other calcination temperatures; it may be due to the selective peak positions 101, 110 and 100 used for the calculations of the percentage phase conversion ratio. It can also be interpreted that higher c/a ratio results highly tetragonal structure which favors ferroelectric property of the materials. Ferroelectric property confirms dielectric nature of the materials. Hence, this discussion supports dielectric behavior of the material

synthesized, which will also be discussed in the forwarding section of electrical measurements.

3.1 Structural and Electrical Characterizations of strontium doped lead titanate

The powders formed were structurally characterized with XRD technique after synthesis, by using the chemically modified solid state reaction and printed on silicon substrate as discussed in the forwarding section of the project. XRD gives information about phase conversion and relative phase conversion for the synthesized PST powders with respect to the standard JCPDS data reported. Crystallite size, c/a ratio and formation of tetragonal structure are also reported. To study the structural aspects FTIR is used for the confirmation of the synthesis mechanism, crystal agglomerations and the grain growth and are reported. The electrical studies were carried for the dielectric nature of the layers deposited. The variation in relative dielectric constant and loss tangent of the selected layers is also studied. Curie-Weiss constant is calculated. Thus, structural and electrical studies of dielectric layers of strontium doped lead titanate is studied.

3.1.1 XRD (X-ray diffraction) Study

The samples were prepared as per the process of synthesis explained in the forwarding section of the project. Figure 3 shows XRD patterns of doped lead titanate calcined at 600^{o}C, 700^{o}C and 800^{o}C respectively for the varying molar concentration of strontium as presented in Table 4. The formation of tetragonal phase is confirmed from the standard JCPDS card file number 01-074-2495 for lead titanate and calculations of anisotropy for XRD peaks of strontium lead titanate. The major peaks have been compared with the standard patterns. Using Debye-Scherer equation, the average crystallite size has been calculated from the experimental XRD peaks. A few unknown miner peaks are also observed in XRD patterns.

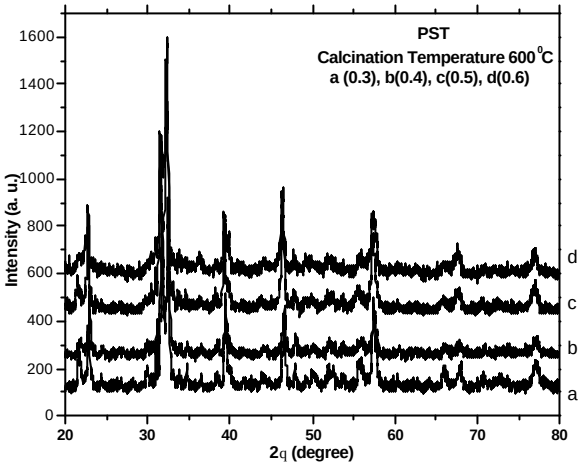

Figure 3: X-Ray Diffraction Patterns for PST annealed in air at 600°C with varying Strontium content in mole a) 0.3 b) 0.4 c) 0.5 d) 0.6

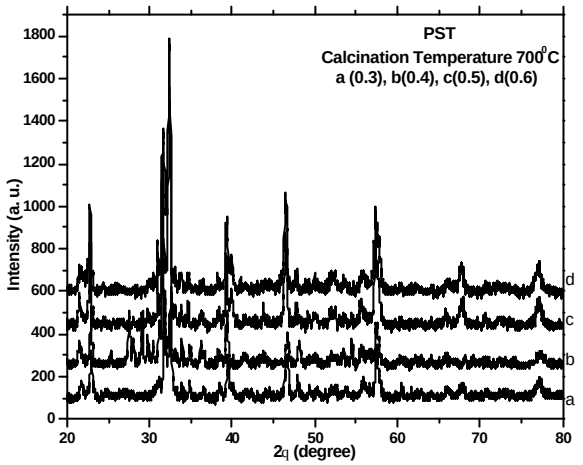

Figure 4: X-Ray Diffraction Patterns for PST annealed in air at 700°C with varying Strontium content in mole a) 0.3 b) 0.4 c) 0.5 d) 0.6

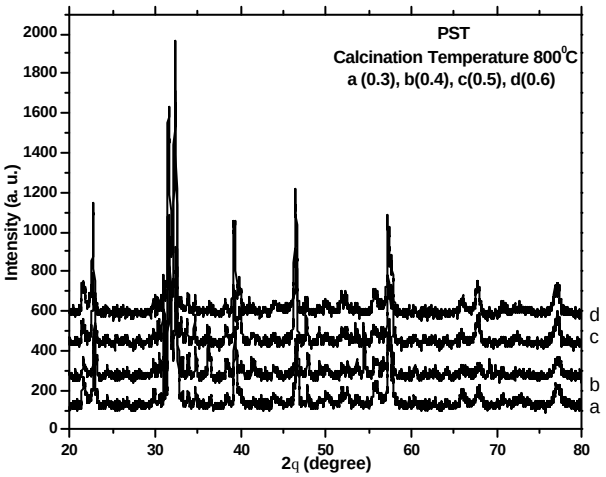

Figure 5: X-Ray Diffraction Patterns for PST annealed in air at 800°C with varying Strontium content in mole a) 0.3 b) 0.4 c) 0.5 d) 0.6

The calculated average crystallite size D vs strontium content in lead titanate is presented in Figure 6. D is calculated for all the molar concentration of Strontium doped lead titanate. The XRD result shows nano-crystalline nature of all the PST powders. These are the plots of crystallite size of the powders with respect to strontium concentration at different calcination temperature. It is also observed that for undoped lead titanate crystallite size is higher i.e. ranging from 71 to 97 nm, while for strontium doped lead titanate is between 13 and 44 nm. Lowest value of the crystallinity is 13 nm for the powder calcined at 600^{o}C and for 6PST. Dependence of the crystalline size on the calcination temperatures is noted. The calcination temperatures for the raw PST white powder, formed during the intermediate stage of the reaction stated in the forwarding section of the project, affects crystalline size as well as properties. The crystallite size is also affected by dopant added. The trend of the crystallite size at 800^{o}C is found to be decreased achieving lowest value 13 nm for molar concentration 0.3. Even though there are different crystallite size with respect to temperature and dopant, it is within the error limit.

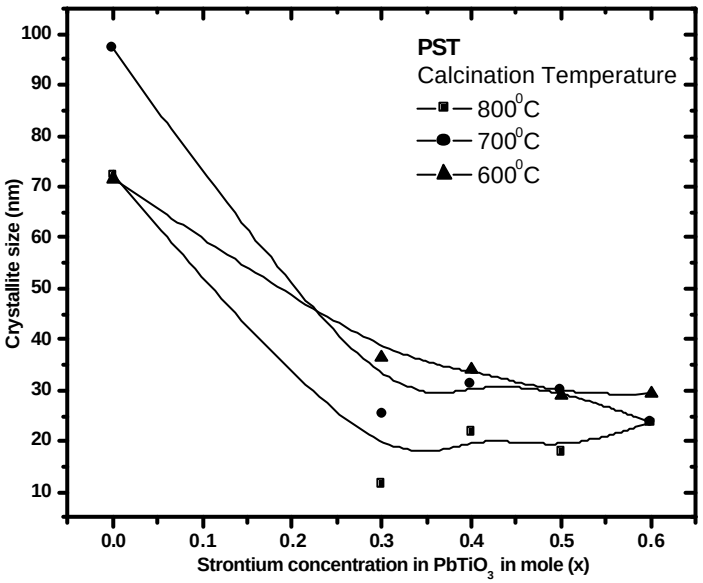

Figure 6: Crystallite size vs calcium content

3.1.2 c/a ratio

X ray diffraction experimental data for strontium doped lead titanate is correlated with the undoped PT calcined at different temperatures presented in the Table 6. Its tetragonal phase is confirmed from the calculations of c/a ratio. Relative % phase conversion ratio is also calculated and presented. At the room

temperature, nano-crystalline PT powder has major peak at (101) which belongs to the tetragonal phase with cell parameters presented in Table 6. Experimentally calculated values of c/a at different calcination temperatures for the PST for varying strontium content is also calculated and presented in Figure 6. For PT c/a ratio is found to be less 1.06152 A^0, 1.05977 A^0, 1.05515 A^0 at 600^{o}C, 700^{o}C and 800^{o}C calcinations respectively.

It increases to maximum value for 0.4 mole concentration of strontium doped in PT, it represents highest tetragonality of 4PST. But, for further increase in the strontium contents, c/a ratio decreases; it is up to the mark to show the tetragonal structure of PST doped up to 0.6 mole concentration of strontium in PT. It means that highly tetragonal structure is formed for specific value of the strontium as dopant [22]. It decreases and then tending toward unity showing phase transition from tetragonal structure to pseudo cubic (c/a for molar concentration 0.6 of strontium in lead titanate is 1.011). Screen printed layers of powders were studied and layers derived from 4PST having comparatively high tetragonal structure to be deposited on the silicon have been reported. It is further studied for its dielectric measurements in the forwarding section of this project.

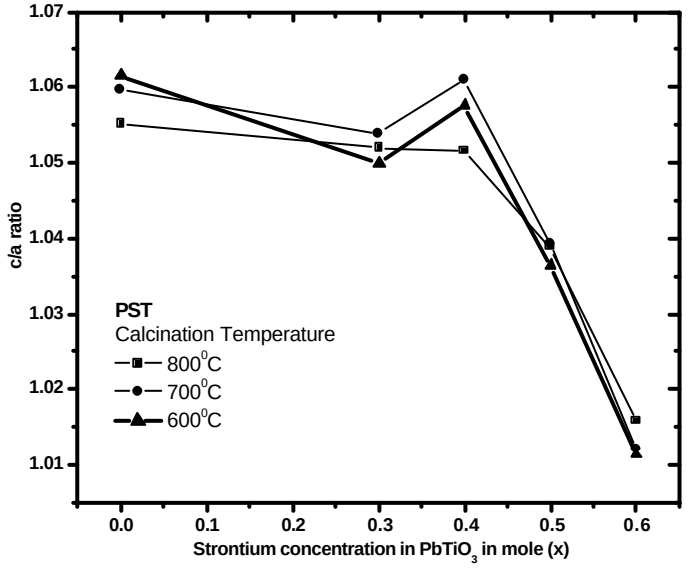

Figure 7: Variation in c/a with respect to calcination concentration at different calcination temperatures.

3.1.3 Relative phase conversion ratio

The major diffraction peaks corresponding to diffraction planes 101, 110 and 100 ascribed to tetragonal $PbTiO_3$ in experimental data as presented in the Figure 1 (e) has been taken for the reference calculations of the phase conversion ratio of the strontium doped lead titanate. The relative % phase conversion of the PST data at different calcination temperature is calculated to that of the data obtained from the characterizations carried out for PT. The relative % phase conversion of PST at different calcination temperatures and doping are shown in Figure 8. It was estimated qualitatively from XRD results using the formula 3.2.

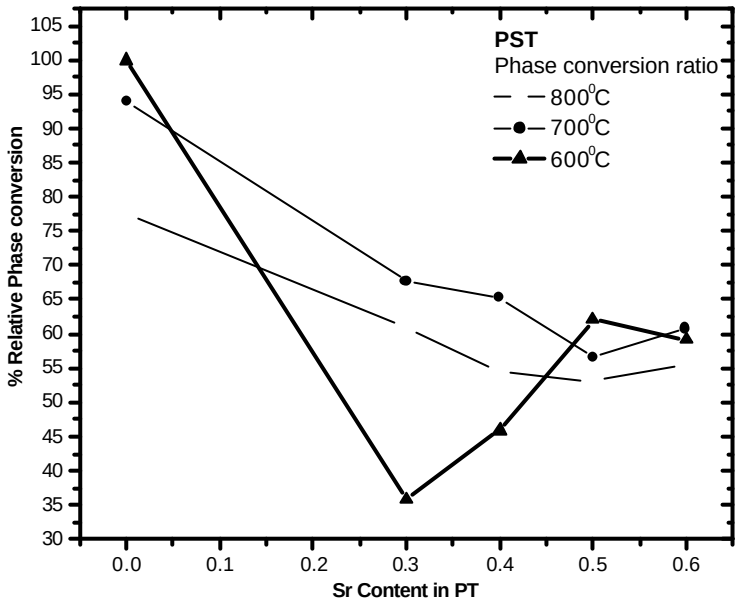

Figure 8: % relative phase conversion w.r.t. Strontium concentration

3.1.4 FTIR (Fourier Transform Infrared Spectroscopy) Study

The samples were prepared as per the process of synthesis explained already. The Figure 9 of FTIR spectra for 4PST, the bands are influenced by substitution of Sr^{+2} in Pb^{+2}. The position of these bands depends on composition [23]. Here the spectra are graphed for selected 4PST composition. Wavelengths of different peaks are observed. The infrared spectra shows sharp peaks for the 4PST700 powders and are medium for 4PST600 and broad in nature for 4PST800. The broad bands are exhibited in the oxide spectra, most probably due to the combination of high degeneracy of vibrational states, thermal broadening of the lattice dispersion band and mechanical scattering from powder samples.

As seen for 4PST 700, the peak around 3510 cm^{-1} is broad in lead-rich and narrow in strontium rich compositions. Normally, lead rich broad peaks and strontium rich sharp peaks are obtained around 3500 cm^{-1}. Broad peaks within the range 1000-1200 cm^{-1} also show strontium rich and 495 cm^{-1} -895 cm^{-1} strontium increasing environment in Pb-Sr-Ti-O composition system. Spectra also shows eliminations of volatile materials formed during the reaction. This discussion supports the formation of 4PST in the stated reaction of the project. The peaks related to O-H, C=N, C=O, C-O and C-C stretches between 1300 cm^{-1} to 1000 cm^{-1} are already discussed in the forwarding section of the project.

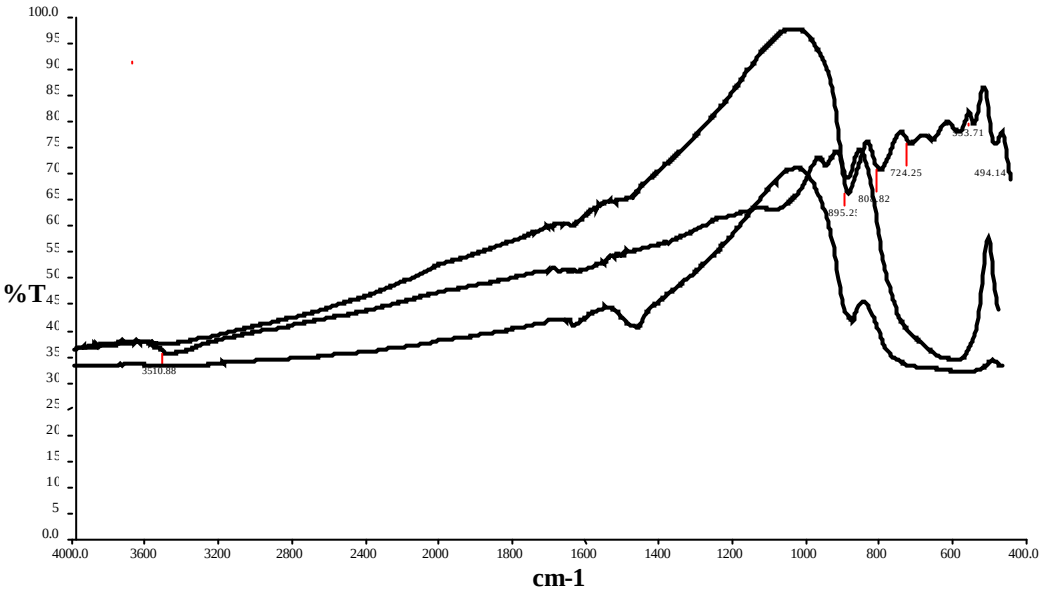

Figure 9: FTIR spectra of 4PST calcined at a) 600^{o}C [top], b) 700^{o}C [middle] and c) 800^{o}C [bottom]

3.1.5 Electrical Measurements

3.1.5.1 Dielectric Study

The films were prepared as per the deposition procedure explained already. Figure 10 shows variation of the dielectric constant and loss with respect to temperature at constant frequency 1 kHz. It is seen that the dielectric constant varies from 246 to 728 within the temperature range 340 to 500^{o}C and decreases for other temperatures including room temperature. The phase transition from tetragonal to pseudo cubic occurs at 340^{o}C for 4PST800 and 4PST700 and 390^{o}C for 4PST600 layers. The dielectric loss factor for the 4PST shows relatively low loss 0.00336 at temperature 390^{o}C, more than room

temperature, but loss is higher 0.00358 at transition temperature 340^{o}C where dielectric constant has high value within the entire temperature range and measurements, it is represented in respective figures 11. As discussed in the next section, ferroelectric and dielectric properties get supported by these observations for electrical measurements.

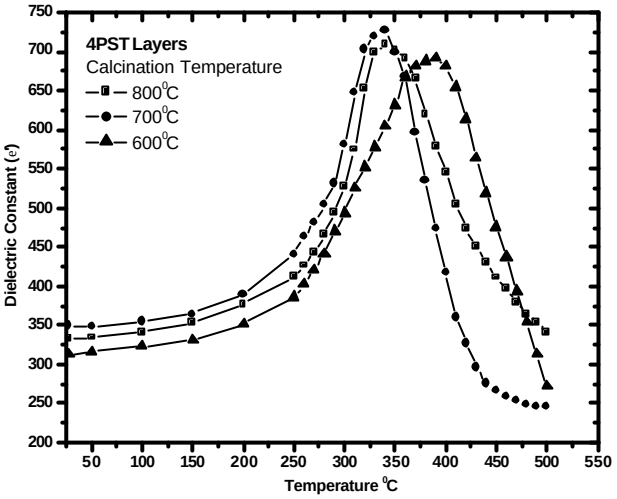

Figure 10: Variation of Dielectric Constant with respect to temperature

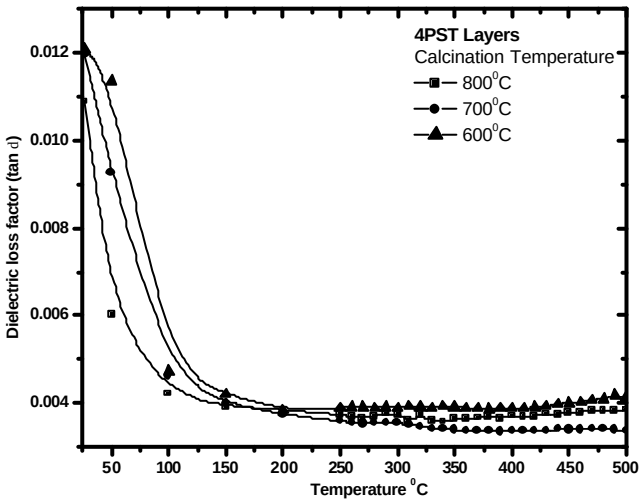

Figure 11: Variation of Dielectric Loss with respect to temperature

3.1.5.2 Curie-Weiss Law

The temperature variation of the dielectric constant for the 4PST700 layer is shown in Figure 10. It is noted that at T_C (Transition temperature) the temperature corresponding to the peak of the dielectric constant is higher. In the

vicinity of the transition temperature, the dielectric stiffness (1/e) follows the well-known Curie-Weiss law as given in the stated equation. Figure 12 shows the temperature behavior of the inverse of the dielectric constant at 1 kHz for the 4PST700 layer. The parameters C and T_O were fitted at a narrow temperature range T_C. From these data, the ferroelectric to paraelectric phase transition temperature i.e. Curie temperature T_C and the Curie-Weiss temperature T_O can be calculated. The fitting parameters are $T_O = 332^oC$ and $C= 5.824 \times 10^3$ K. The fact showing the Curie-Weiss temperature ($T_O = 332^oC$) lower than the transition temperature ($T_O = 340^oC$) is expected from the first order phase transition between the paraelectric and ferroelectric phases [24-27]. Similar behavior for the 4PST600 and 4PST800 layers is depicted in Table 8.

Layer	e	**T_O**	**T_C**	**C**
4PST600	688	377	390	8944
4PST700	728	332	340	5824
4PST800	709	337	340	2127

Table 8: Layers deposited and Curie-Weiss Constant

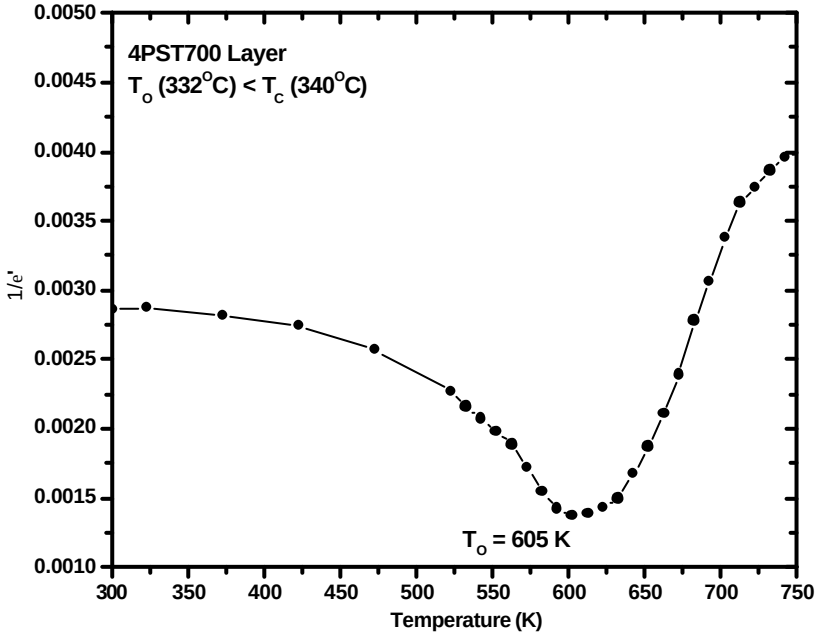

Figure 12: Inverse of dielectric constant as a function of temperature

4. Conclusions

Structural and electrical characterization for the strontium doped lead titanate for 0.4 mole concentration of strontium and at varying calcination temperatures is successfully studied with its layering by screen printing on silicon (111) substrate.

XRD confirms crystallite size of about 13 nm along with tetragonal structure. c/a ratio calculated shows lattice anisotropy and hence tetragonal structure of strontium doped lead titanate. The highest value of c/a for 0.4 molar concentration of strontium strongly agreed to get tetragonal phase conversion of the strontium doped lead titanate with respect to undoped lead titanate as discussed. Higher tetragonality is occurred at 0.4 mole of strontium. The calculated relative % phase conversion ratio for the tetragonality is 99.88% which justifies its phase purity.

FTIR spectra show lead rich and strontium rich frequency effects at around 3500 cm^{-1}, broadness in the spectra shows thermal broadening range to justify diffusivity.

The higher values of dielectric constant as compare to the undoped and calcium doped lead titanate are observed. The 4PST screen printed layers on Si (111) at 1 kHz, has high dielectric constant 728 with relatively low loss of 0.00336 at 340^{o}C.

5. Future Scope

The area of dielectrics has very interesting features with respect to the development and advancement of new materials for various device applications. Lead titanate ($PbTiO_3$) with and without doping exhibit many attractive properties. These attributes make them attractive for devices in many electronic applications in the form of bulk, thin-thick film, composite and single crystal. These applications include ceramic capacitor, surface acoustic wave (SAW) devices, actuators and piezoelectric transducer etc. Recently Its applications in pyro-electric devices, ferroelectric memories, smart materials, pressure sensors and hydrophones are greatly accounted due to high speed, low power consumption, high dielectric constant, etc.

Further extension of work can also be done by refinements and modifications in experimental part, providing the varying temperature-pressure effects. It was found that domain study of ferroelectric materials is also the important issue. Dependence of grain size and other properties on sintering temperature can be studied. Focus can be given on piezoelectric, pyroelectric properties of it. At the same time other materials can also be developed in bulk, thin-thick film and in the form of devices to be used for the human world.

In future, with this parallel thinking, many materials and methods are kept in mind and have planned to study and to develop the devices which will contribute the science world for the relevance of the research community and the society.

References

[1] Gnade B, Summerfelt SR, Crenshaw D, Science and Technology of Electro ceramics Thin Films, NATO ASI Series, ed. O Auciello, R Waser, 284 (1995) 373

[2]. Kotecki DE., Integ. Ferroelec. 16 (1995) 1

[3] J. F. Scott, Annu. Rev. Mater. Sci. 28 (1998) 79

[4] H. Altenburg, J. Plewa, G. Plesch, O. Shpotyuk Pure Appl. Chem., 74 (11) (2002) 2083

[5] W. Vermeirsch, Microelectronics International 1 (1) (1982) 11

[6] A.J. Moulson, J.M. Herbert, Electrceramics –materials, properties, applications.

[7] M.S. Vijaya, G. Rangarajan Materials Science, Tata Mcgraw-Hill

[8] Anthony R. West, "Solid State Chemistry and its Applications", Wiley and Sons (2005)

[9] B. Gerand, G. Nowogrocki, J. Guenot, M. Figlarz, "Preparative methods in Solid State Chemistry", Academic press, York, USA (1979) 1936.

[10] Wojciech L. Suchanek and Richard E. Riman, Advances in Science and Technology Vol. 45 (2006) 184.

[11] B. B. He, Introduction to two-dimensional X-ray diffraction, Powder Diffraction, Vol. 18, No 2 (2003)

[12] Als-Nielsen, J., McMorrow, D., Elements of Modern X-Ray Physics,

Wiley, (2001)

[13] X. Chen, H. Fan, L. Liu, J. Cryst. Growth 284 (2005) 434

[14] J. A. Owczarek and F. L. Howland. IEEE 13 (1990) 358.

[15] D. E. Riemer. Solid State Tech. 85 parts I/II (1988) 107.

[16] J. Pan, G. L. Tonkay, A. Quintero. International Symposium on Microelectronics (1998) 264.

[17] Patterson, A.L., The Scherrer Formula for X-Ray Particle Size Determination, PRL, Vol.56 (1939) 978

[18] A. Udomporn, S. Ananta. Materials Letters 58 (2004) 1154.

[19] M. M. Rashad, R. S. Mohammed, M. M. Hessien, I. A. Ibrahim, A. T. Kandil, J. Opto. Ele. Adv. Mat., Vol. 10 (5) (2008) 1026

[20] Mark A. McCormick1, Elliott B. Slamovich, Journal of the European Ceramic Society 23 (2003) 2143

[21] A. Beitollahi, S. M. Bafghi, S. M. A. Jazayeri Dezfouli, H. Ghanbari, J Mater Sci: Mater Electron 17 (2006) 361

[22] K. M Nair, J. P. Guha and A. Okamoto, Ameri. Ceram. Soc, 32 (1993) 145

[23] C. R. Gautam, D. Kumar, Om Parkash, Bull. Mater. Sci., 33 (2) (2010) 145

[24] S.H. Leal, F.M. Pontes, E.R. Leite, E. Longo, P.S. Pizani, A.J. Chiquito, M.A.C. Machado, J.A. Varela, Mat. Chem. Phys. 87 (2004) 353

[25] F. M. Pontes, S. H. Leal, E. R. Leite, E. Longo, P. S. Pizani, A. J. Chiquito, J. A. Varela, J. App. Phys. 96 (2) (2004) 1192

[26] S. Normura and S. Sawada, J. Phys. Soc. Jpn. 10, (1955) 108

[27] Bajpeyee A. U., Ph. D. thesis, Sant Gadge Baba Amravati University, Amravati, Maharashtra (INDIA) 444 606

*****